

# SHEAR ANALYSIS FOR D-REGION IN RC MEMBERS CONSIDERING LOCALIZATION IN COMPRESSION

Manakan LERTSAMATTIYAKUL<sup>1</sup>, Junichiro NIWA<sup>2</sup>,  
Torsak LERTSRISAKULRAT<sup>3</sup> and Tomohiro MIKI<sup>1</sup>

<sup>1</sup>Member of JSCE, Ms. Eng., Graduate Student, Dept. of Civil Eng., Tokyo Institute of Technology  
(2-12-1 O-okayama, Meguro-ku, Tokyo 152-8552, Japan)  
E-mail: 96b31110@cv.titech.ac.jp

<sup>2</sup> Fellow of JSCE, Dr. Eng., Professor, Dept. of Civil Eng., Tokyo Institute of Technology

<sup>3</sup> Member of JSCE, Ph. D., Former Graduate Student, Dept. of Civil Eng., Tokyo Institute of Technology

It is usually observed that RC deep beams, where the entire member becomes D-region, fail by the localized compressive failure of concrete. In this study, the utilization of the concept on localized compressive failure in formulation of the material model of concrete, based on the parameters such as the localized compressive failure length,  $L_p$ , and the compressive fracture energy,  $G_{Fc}$ , is performed. By incorporating the proposed compressive stress-strain relationship to the 2 simplified analytical models, the lattice model and Mander's truss model, the satisfactory predictions on the shear behavior of RC deep beams with and without transverse reinforcement are obtained.

*Key Words* : D-region, RC deep beam, localized compressive failure, lattice model, Mander's truss model

## 1. INTRODUCTION

In complex civil engineering structures, the discontinuities such as the abrupt changes in cross-sectional dimensions or the presence of concentrated loads or reactions, which cause disturbances in the flow of internal forces, are usually observed. These kinds of disturbances in the flow of internal forces around the discontinuities result in what is called *disturbed region* or *D-region*<sup>1)</sup>. This can be observed in such a structure as RC deep beams, where the entire member becomes D-region because of its comparatively low shear span to effective depth ratio,  $a/d$ , which is less than or equal to 1. In RC deep beams subjected to concentrated loading, the force is transmitted directly to the supports by the concentrated unidirectional compressive stresses as the bulging struts. Thus, due to these stresses, the flow of internal forces becomes not uniform over the whole region of RC deep beams. As a result, the state of stresses cannot be derived section by section from the sectional effects (i.e. moment, axial force and shear force), as is normally in the case for RC slender beams, whose effective depth is small compared with

their shear span. Therefore, the design and prediction of the behavior of RC deep beams are more difficult than those of RC slender beams.

At the ultimate stage of RC deep beams, along the diagonal cracks connecting the loading point and supports, the failure characterized by crushing of concrete, at the upper portion of a beam in the vicinity of the loading point, is usually observed<sup>2)</sup>. It implies that, due to the disturbances of concentrated stresses as D-region in RC deep beams, the failure is localized called as the localized compressive failure of concrete. In order to obtain more accurate prediction on the shear behavior of RC deep beams, not only the concept of compression softening due to the increase in transverse tensile strain<sup>3)</sup>, but the concept of localized compressive failure of concrete should also be incorporated. In this research, the localized compressive failure length,  $L_p$ , and the compressive fracture energy,  $G_{Fc}$ , proposed in the previous study<sup>4)</sup> have been applied to formulate the stress-strain relationship of concrete in compression.

In this study, two analytical methods named the lattice model and Mander's truss model are selected. The lattice model is considered as a simplified analytical model to clarify the shear resisting

mechanism of RC beams<sup>5</sup>). Alternatively, Mander's truss model is the updated truss model with a smaller number of degree of freedom compared with the lattice model. And it can be used to assess the shear behavior of RC members by considering the interaction between the shear and flexure mechanisms. Similar to the traditional truss models, the resistances are evaluated from the contributions of transverse reinforcement and tensile concrete in the shear mechanism. As the outstanding point of this model, by applying the virtual work method and the numerical integration scheme such as Gauss quadrature, the relationship of shear force and its deformation can easily be derived<sup>6</sup>.

In order to clarify the overall shear behavior of D-region in RC members, the RC deep beam, where its whole member is included into D-region by the concentrated loading, was selected as the target in this analytical study. In this paper, the lattice model and Mander's truss model incorporating the concept of localized compressive failure have been utilized to evaluate the shear behavior of RC deep beams where effective depth,  $d = 400$  and  $600$  mm with the variation of transverse reinforcement ratio,  $r_w = 0, 0.42$  and  $0.84\%$ <sup>2</sup>).

## 2. LATTICE MODEL ANALYSIS

### (1) Fundamental principles

Figure 1 illustrates the schematic diagram of the lattice model in which a RC beam is modeled into an assembly of the truss components. The concrete is modeled into flexural compression members, flexural tension members, diagonal compression members, diagonal tension members, vertical compression members and an arch member. The modeling of reinforcements consists of horizontal and vertical members. The diagonal compression and the diagonal tension members have an inclination of  $45^\circ$  and  $135^\circ$ , respectively. The major remarkable points of the lattice model is to consider the concrete diagonal tension member and the arch member, which provide more appropriate prediction on the shear behavior of concrete beams before and after the initiation of the diagonal cracking.

### (2) Modeling of each member

As shown in Fig. 2, the web concrete is divided into truss and arch parts. By assuming the parameter  $t$  as the ratio of the width of the arch member to the beam width,  $b$ , the widths of the arch member and the truss member are respectively equal to  $bt$  and  $b(1-t)$ , where  $0 < t < 1$ . The value of  $t$  is determined in such a

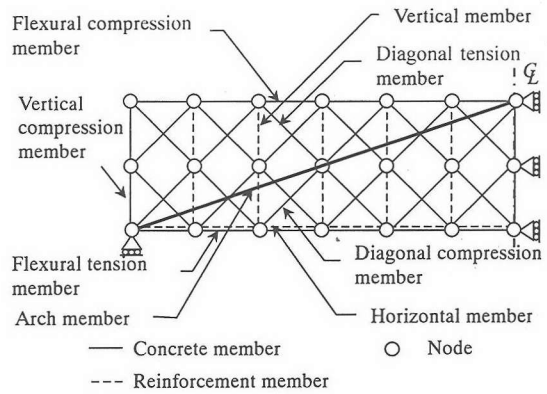


Fig.1 Schematic diagram of RC beam in the lattice model (with transverse reinforcement)

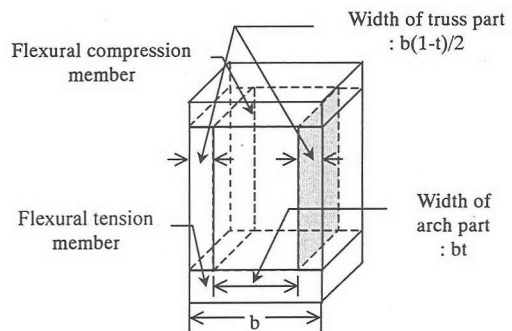


Fig.2 Cross section of RC beam in the lattice model

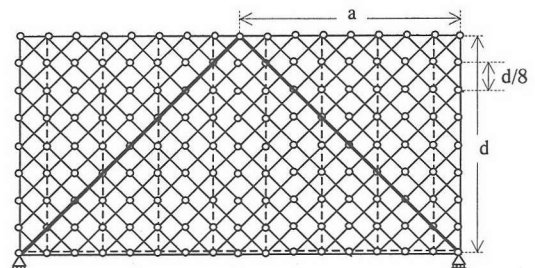


Fig.3 Complete model of RC deep beam in the lattice model (with transverse reinforcement)

way that it minimizes the total potential energy of the entire structure. The total potential energy is calculated from the summation of the strain energy of each member and the work done by externally applied load based on the elastic analysis.

By considering the mesh discretization and the complexity of flow of internal forces in the member, a RC deep beam was suitably modeled in the complete model in which the vertical spacing of adjacent 2 nodes is equal to  $d/8$  and the value of  $a/d$  is equal to 1.0 matching to the actual specimen as depicted in Fig. 3. Based on the previous study<sup>7</sup>, the arch member is considered to connect between the

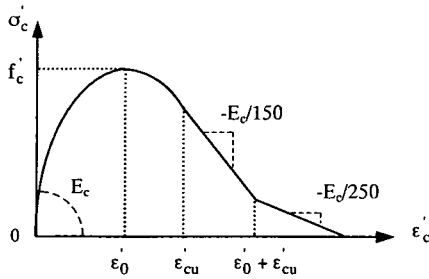


Fig.4 Compression model

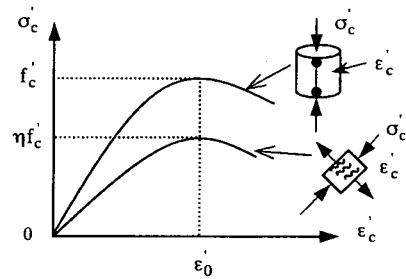


Fig.5 Compression softening model

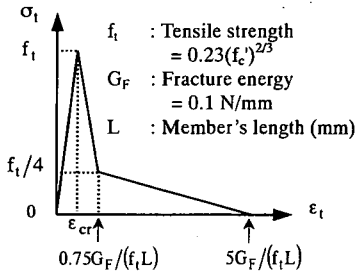


Fig.6 One-forth model

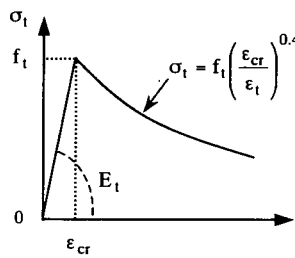


Fig.7 Tension stiffening model

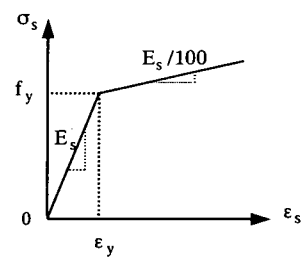


Fig.8 Bilinear elasto-plastic model

loading point and the support with the thickness assumed to be  $(0.3d+r) \sin 45^\circ$ , where  $r$  is the width of a bearing plate. The thickness of the diagonal members is assumed to be  $(d/8) \sin 45^\circ$ . The length of the diagonal members and the arch member are equal to  $d/(8 \sin 45^\circ)$  and  $d/\sin 45^\circ$ , respectively.

### (3) Material model of each member

It is known that, after the cracks occurred, the compression concrete members show the softening of their stress-strain relationship due to the transverse tensile strain<sup>3</sup>. Hence, for the diagonal compression members and the arch member, by taking into account the strain of their perpendicular diagonal tension members,  $\epsilon_t$ , the compressive stress-strain relationship under the biaxial stress state proposed by Vecchio and Collins<sup>3</sup> (Figs. 4 and 5) is applied as;

$$\sigma'_c = \eta f'_c \left[ 2 \left( \frac{\epsilon'_c}{\epsilon'_0} \right) - \left( \frac{\epsilon'_c}{\epsilon'_0} \right)^2 \right] \quad (1)$$

where

$$\eta = \frac{1}{0.8 + 0.34(\epsilon_t/\epsilon'_0)} \leq 1.0, \quad \epsilon'_0 = 0.002$$

As depicted in Fig. 4, after the ultimate strain,  $\epsilon'_{cu} = 0.0035$ , to reduce the stiffness of the member, the bilinear model was applied. It is noted that, for simplicity, the compressive stress and strain are considered in positive values.

For the flexural and vertical compression members, the compression softening parameter,  $\eta$ , is assumed to be equal to 1.0.

After the crack occurring, the tension softening model named the one-forth model is employed as the material model for the diagonal tension members as shown in Fig. 6. By considering the bond between concrete and the longitudinal reinforcement, the tension stiffening model is applied to the flexural tension members as depicted in Fig. 7. For all reinforcements, the bilinear elasto-plastic model of steel is used (Fig. 8).

## 3. MANDER'S TRUSS MODEL ANALYSIS

Mander's truss model is the updated truss model with a small number of degree of freedom, which can be used to evaluate the relationship of shear force and deformation based on the concept of the combination of shear and flexure mechanisms<sup>9</sup>. The total deformation of the member can be expressed in terms of 2 deformation components as:

$$\Delta = \Delta_v + \Delta_f \quad (2)$$

where  $\Delta$ ,  $\Delta_v$  and  $\Delta_f$  are total, shear and flexure deformations of a RC member, respectively.

And the shear resistance should be the lesser of:

$$V_v = V_s + V_c \quad \text{and} \quad V_f = \frac{M_y}{L} \quad (3)$$

where  $V_v$  and  $V_f$  are correspondingly referred to the shear force resisted by shear and flexure mechanisms.  $V_s$  and  $V_c$  are the shear resistances due to the contributions of transverse reinforcement and tensile concrete, respectively.  $M_y$  is the yielding moment of the RC member.

In the modeling of concrete web width for models of  $V_s$  ( $b_s$ ) and  $V_c$  ( $b_c$ ), by performing in the same fashion as the lattice model, the ratio of the model width which minimizes the potential energy is determined to give a good prediction.

### (1) Shear mechanism

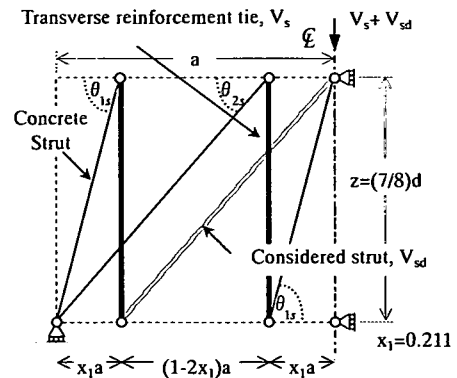
To evaluate  $V_s$  and  $V_c$  in the shear mechanism, one half of a RC deep beam was modeled by applying two-point Gauss quadrature with the normalized coordinate parameter,  $x_1$ , to Mander's truss model, as depicted in Figs. 9(a) and (b)<sup>6)</sup>. In the model of  $V_s$ , the transverse reinforcements (bold black lines) are modeled perpendicularly to the beam axis. In the model of  $V_c$ , the inclined concrete ties (bold black lines) are modeled correspondingly to the ineffective zones in which the effects of a concentrated load and supports in these regions should be eliminated. The diagonal struts characterize the concrete compression field stabilizing the truss models. In the conventional truss model, the shear resisting capacity is assessed from the summation of the shear resistances due to the transverse reinforcement ties in Fig. 9(a),  $V_s$ , and the inclined concrete ties in Fig. 9(b),  $V_c$ , while the shear force resisted by the strut along the diagonal cracks is neglected. However, for RC deep beams, the arch action, which is created from the diagonal cracks and longitudinal reinforcement, becomes the significant resistance in governing the failure mechanism after the occurring of the diagonal crack. Consequently, the shear resistances due to the concrete struts that transmit the forces along the diagonal crack should be taken into the consideration. From the configuration of Mander's truss model (Fig. 9) and the experimental observation that the localization in compression usually takes place in the vicinity of the loading point, the struts connecting the loading point and the node locating next to the support were suitably selected and called as the *considered struts*, (gray bold lines in the both models). The shear resistance due to the considered struts in the models of  $V_s$ ,  $V_{sd}$ , and in the models of  $V_c$ ,  $V_{cd}$ , should be taken into account. The equations of  $V_{sd}$  and  $V_{cd}$  were derived by using the equilibrium and compatible conditions in the diagonal struts<sup>6)</sup>. The expressions of shear resistance can be rewritten as:

$$V_v = V_s + V_c + V_{sd} + V_{cd} \quad (3)$$

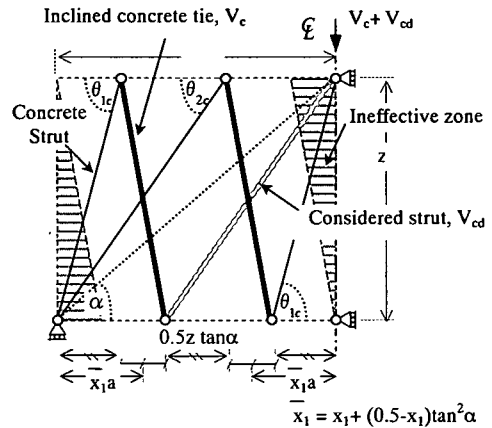
where

$$V_s = A_{st} \sigma_s (\epsilon_s) \frac{z}{s} \cot \theta \quad (3a)$$

$$V_c = \sigma_t (\epsilon_t) A_v \cot \theta \cos 2\theta \quad (3b)$$



(a) Model of  $V_s$



(b) Model of  $V_c$

Fig.9 Modeling of RC deep beam in Mander's truss model

$$V_{sd} = \frac{\sigma'_c (\epsilon'_c) A_v (b_s/b) \cot \theta}{2(1+x_2^2 \cot^2 \theta)} \quad (3c)$$

$$V_{cd} = \frac{\sigma'_c (\epsilon'_c) A_v (b_c/b) \tan \theta (1 - \tan^2 \theta)}{2 \left[ (1 - \tan^2 \theta)^2 x_2^2 + \tan^2 \theta \right]} \quad (3d)$$

where  $\sigma_s$  : average tensile stress of transverse reinforcement,  $\sigma_t$  : average tensile stress of concrete ties,  $\sigma'_c$  : compressive stress of the considered strut,  $A_v = bz$ ,  $A_{st}$  : cross-sectional area of the transverse reinforcement,  $s$  : spacing,  $\theta$  : crack angle,  $x_2 = 1 - x_1$ .

The crack angle is simply set to be equal to  $\alpha = \tan^{-1}(z/a)$  for RC deep beams without transverse reinforcement. For RC deep beams with transverse reinforcement, the crack angle can be determined from Eq. 4 proposed by Mander, et al.<sup>6)</sup>

$$\theta = \tan^{-1} \left\{ \left[ r_w n + \zeta \left( \frac{r_w A_v}{p_i A_g} \right) \right] / (1 + r_w n) \right\}^{1/4} \quad (4)$$

where  $A_g = bd$ ,  $p_t = A_s/A_g$ ,  $n = E_s/E_c$ ,  $\zeta$  : boundary condition constant = 1.5704,  $A_s$  : cross-sectional area of the longitudinal reinforcement, and  $r_w = A_{st}/(bs)$ .

In both models, the rigid longitudinal chords are assumed in the analysis in order to neglect the effect of flexural deformation. As the advantage point of Mander's truss model compared with other contemporary truss models, by utilizing the virtual work method for the model, the relationships between the deformation and each shear resisting component can be derived.

## (2) Flexure mechanism

Prior to the onset of flexural crack, the rigidity of the flexural concrete should be considered as shown in Fig. 10. With the increase in moment, the flexural rigidity of the section is reducing by cracking of concrete. After the flexural cracking moment,  $M_{cr}$ , was reached, the behavior of the section is assumed to depend mostly on the reinforcement content. The way of calculation is summarized as follows.

In case of  $M < M_y$  : The curvature of the beam,  $\phi$  :

$$\phi = \frac{3\Delta_f}{L^2} \quad (5)$$

$$M = \phi E_c I \quad (6)$$

$$\text{If } M \leq M_{cr} : I = I_g = \frac{bh^3}{12} \quad (7)$$

$$\text{If } M > M_{cr} : I = \left(\frac{M_{cr}}{M}\right)^4 I_g + \left(1 - \left(\frac{M_{cr}}{M}\right)^4\right) I_{cr} \quad (8)$$

$$\text{where } M_{cr} = f_b \frac{bh^2}{6} \quad (9)$$

$$I_{cr} = \frac{bx^3}{3} + n[A'_s(x-d')^2 + A_s(d-x)^2] \quad (10)$$

$$x = -\frac{n(A_s + A'_s)}{b} + \sqrt{\left[\frac{n(A_s + A'_s)}{b}\right]^2 + \frac{2n}{b}(A_s d + A'_s d')} \quad (11)$$

$I_{cr}$  : moment of inertia neglecting the concrete portion in tension,  $f_b$  : flexural strength,  $h$  : member's height,  $A'_s$  : cross-sectional area of compression steel,  $d'$  : distance from the extreme compression fiber to the centroid of, compression steel and  $x$  : distance from the extreme compression fiber to the neutral axis. The iteration process is applied to obtain  $M$  from Eqs. 6 and 8.

In case of  $M \geq M_y$  : For simplicity,  $M$  is set to be equal to  $M_y$ . Subsequently, from the obtained  $M$ ,  $V_f$  can be evaluated by dividing  $M$  with  $L$ . Finally, the relationship between  $V_f$  and  $\Delta_f$  can be obtained.

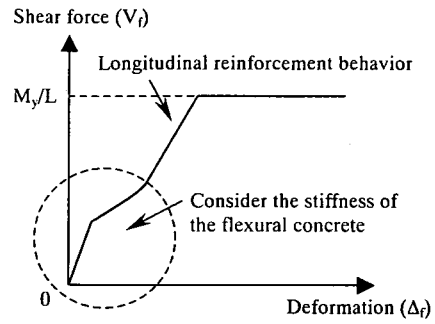


Fig.10 Shear force ( $V_f$ ) – deformation relationship

## 4. COMPRESSIVE STRESS-STRAIN CURVE BASED ON THE CONCEPT OF LOCALIZED COMPRESSIVE FAILURE OF CONCRETE

In the conventional lattice model, the parabolic compressive stress-strain relationship including the consideration of compression softening proposed by Vecchio and Collins<sup>3</sup> is adopted as shown in Fig. 5. Since the failure in RC deep beams is localized after the peak load was reached, the externally applied energy is intensively consumed by the concrete in the localized failure zone. To assess the post-peak path of shear behavior of RC deep beams correctly, the descending branch of compressive stress-strain curve should be modified by considering the localized compressive failure. The localized compressive failure volume in RC deep beam,  $V_p^d$ , and the compressive fracture energy in RC deep beam,  $G_{Fc}^d$ , will be determined based on the concepts of  $L_p$  and  $G_{Fc}$  in the uniaxial compression as follows<sup>4</sup>.

### (1) $V_p^d$ and the volume amplification factor, $K_V$

As demonstrated in the previously studied uniaxial compression tests<sup>4</sup>, the localized compressive failure volume,  $V_p$ , can be obtained from  $L_p$  multiplied by  $A_c$  where  $A_c$  is the cross-sectional area of the specimen.

On the other hand, for the RC deep beams in which the localized compressive failure occurred (i.e. the beams where  $d = 400$  and  $600$  mm with  $r_w$  of 0, 0.42 and 0.84%)<sup>2</sup>, the failure volume increased due to the effects of transverse reinforcement. Therefore, the ratios of  $V_p^d$  of the beams with transverse reinforcement to those without transverse reinforcement, so called the volume amplification factors,  $K_V (\geq 1)$ , were calculated and summarized in Table 1 (Fig. 11). Here, the determination of dimension of concrete failure volume along the arch member was considered as follows. For the

Table 1 Values of  $K_V$  and  $K_E$

Specimen	d (mm)	$r_w$ (%)	$K_V$	$K_E$	$K_V/K_E$
D400	400	0.00	1.00	0.87	1.15
D404		0.42	1.78	0.89	2.00
D408		0.84	1.56	0.81	1.93
D600	600	0.00	1.00	0.89	1.12
D604		0.42	1.33	0.78	1.71
D608		0.84	1.48	0.89	1.66

cross-sectional area, the width and the thickness of the member were assumed to be  $(0.3d+r) \sin 45^\circ$  and  $b$ , respectively. The values of  $L_p$  in RC deep beams,  $L_p^d$ , were determined as the lengths of the portion where the locally consumed energy is larger than the empirical criterion obtained in the previous study<sup>2)</sup>.

(2)  $G_{Fc}^d$  and the energy reduction factor,  $K_E$

The compressive fracture energy,  $G_{Fc}$ , is defined as the energy required to cause the compressive failure per unit volume of failure concrete. In the uniaxial compression,  $G_{Fc}$  can be calculated by dividing the externally applied energy that causes failure of the specimen,  $E_{ext}$ , by  $V_p$  as:

$$G_{Fc} = \frac{E_{ext}}{V_p} \quad (12)$$

For the  $G_{Fc}^d$  of RC deep beams, the energy consumed by the failure concrete in a beam should be evaluated first. Unlike the uniaxial compression tests, the effects of the friction between the loading plates and the beam together with the stress conditions inside the beam should be considered. It was observed from the previous study that, although the magnitude of locally consumed energy in the vicinity of the loading plates was relatively high, the local stress-strain distribution did not show the softening behavior<sup>2)</sup>. In other words, it did not fail. Therefore, the fraction of the externally applied energy consumed in the portion which was not judged to fail (intact zone along both arches) should be taken into account. In order to approximate the energy absorbed solely by the failure zone, the energy reduction factor,  $K_E (\leq 1)$ , is introduced as the ratio of the energy consumed in the failed portion to the energy totally consumed by the compressive arches (both sides)<sup>2)</sup>. Hence, the energy that caused the failure to concrete,  $E_{net}^d$ , can be calculated from Eq. 13 (Fig. 12).

$$E_{net}^d = K_E (E_{ext} - E_{yield}) \quad (13)$$

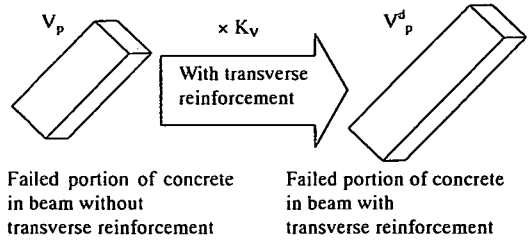


Fig.11 Concept of volume amplification factor;  $K_V$

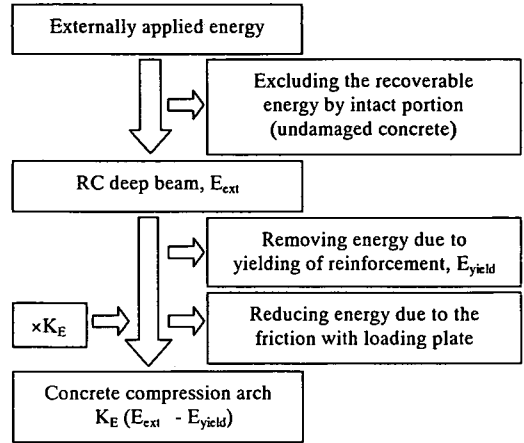


Fig.12 Concept of the energy reduction factor;  $K_E$

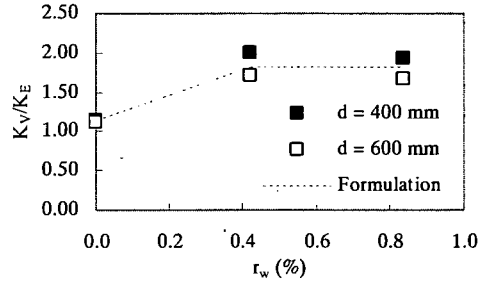


Fig.13 Formulation of  $K_V/K_E$

where  $E_{ext}$  : the total externally applied energy and  $E_{yield}$  : energy consumed by yielded reinforcements for the beams with transverse reinforcement.

(3) Formulation of  $K_V/K_E$

The results of  $K_V/K_E$  for each RC deep beam are plotted in Fig. 13. Since the experimental data are limited, the formulation of numbers of  $K_V/K_E$  to be applied in the analysis is quite difficult. Therefore, the values of  $K_V/K_E$  are simply assumed, regardless the effective depth, to be equal to 1.14 and 1.82 for RC deep beams without and with transverse reinforcement, respectively, as summarized in Eq. 14. These obtained parameters will be used in the following section.

$$\frac{K_V}{K_E} = 1.14 ; \text{ beam without transverse reinforcement}$$

$$= 1.82 ; \text{ beam with transverse reinforcement} \quad (14)$$

#### (4) Application of the localized compressive failure concept to the compressive stress-strain relationship

For concrete members with the cross-sectional area  $A_c$  and subjected to uniaxial compression, the localized compressive fracture length,  $L_p$ , can be determined by Eq. 15<sup>4</sup>.

$$\frac{L_p}{D^*} \begin{cases} = 1.36 & ; D^* < 100 \\ = -3.53 \times 10^{-5} D^{*2} + 1.71 & ; 100 \leq D^* \leq 180 \\ = 0.57 & ; D^* > 180 \end{cases} \quad (15)$$

where  $D^* = \sqrt{A_c}$  (mm).

Subsequently, the localized compressive failure volume,  $V_p$ , can be obtained from  $L_p$  multiplied by  $A_c$ . Hence,  $V_p^d$  of RC deep beams can be calculated as:

$$V_p^d = K_V \times V_p \quad (16)$$

It has been proved that the compressive fracture energy obtained from the RC deep beam tests,  $G_{Fc}^d$ , is equivalent to  $G_{Fc}$  from the uniaxial compression tests and can be evaluated from the empirical equation in terms of  $f_c'$  as expressed in Eq. 17<sup>2</sup>.

$$G_{Fc} = G_{Fc}^d = 0.086 f_c'^{1/4} \quad (\text{N/mm}^2) \quad (17)$$

By knowing  $V_p^d$ , the energy consumed by the failure portion of concrete,  $E_{net}^d$ , can be obtained as the product of  $G_{Fc}^d$  and  $V_p^d$ . Referring to the concepts explained in section 4(2), the energy totally consumed in the compression arch inside the RC deep beams,  $E_T^d$ , which is equivalent to the area under the load-deformation relationship ( $P-\Delta$ ), should be calculated from the theoretical value of  $E_{net}^d$  divided by the factor  $K_E$  as expressed in Eq. 18.

$$E_T^d = E_{net}^d / K_E = (G_{Fc}^d \times V_p^d) / K_E \quad (18)$$

From Eq. 16,

$$E_T^d = (G_{Fc}^d \times V_p) \times (K_V / K_E) \quad (19)$$

The empirical factor,  $K_V / K_E$  is applied in this step. Finally, from Eq. 17,

$$E_T^d = (G_{Fc} \times V_p) \times (K_V / K_E) \quad (20)$$

In order to apply this concept into the material model of concrete in compression,  $E_T^d$  should be transformed to energy per unit volume,  $e_T^d$ , which is equal to the area under the compressive stress-strain relationship ( $\sigma - \epsilon$ ) as shown in Eq. 21.

$$e_T^d = \int \alpha d\epsilon = \int_0^L \frac{P}{A_c} \frac{d\Delta}{L} = \frac{E_T^d}{V_c}$$

$$= \frac{G_{Fc} V_p}{V_c} \frac{K_V}{K_E} = \frac{G_{Fc} L_p}{L} \frac{K_V}{K_E} \quad (21)$$

where  $V_c = A_c \times L$ ,  $L$  is the member's length.

#### (5) Formulation of the stress-strain relationship

Based on the obtained parameters, the stress-strain relationship for compression members can be proposed as depicted in Fig. 14. For the ascending branch (pre-peak), the parabolic relationship with the consideration of compression softening proposed by Vecchio and Collins<sup>3</sup>) has been applied. The descending branch (post-peak) was modeled into two straight lines, *Line A* and *Line B*, for simplicity. In order to express the behavior of cracked reinforced concrete in compression<sup>3</sup>),  $\eta$  is also incorporated in the descending branch of the stress-strain relationship. Finally, the formulation for the stress-strain relationship has been proposed as summarized in Eq. 22.

$$\sigma_c' = \eta f_c' \left[ 2 \left( \frac{\epsilon_c'}{\epsilon_0'} \right) - \left( \frac{\epsilon_c'}{\epsilon_0'} \right)^2 \right] ; \quad \epsilon_c' \leq \epsilon_0' \quad (a)$$

$$= \eta (A_1 \epsilon_c' + A_2) ; \quad \epsilon_0' < \epsilon_c' \leq \epsilon_{last}' \quad (b)$$

$$= \eta (B_1 \epsilon_c' + B_2) ; \quad \epsilon_{last}' < \epsilon_c' \quad (c)$$

$$(22)$$

From Fig. 14, the totally consumed energy,  $e_T^d$ , is equal to the summation of area under the ascending branch,  $e_1$ , and the descending branch,  $e_2$ . Here,  $e_1$  can be obtained by integrating Eq. 22a up to the peak point as shown in Eq. 23. Because the value of  $\eta$  is depending on the value of the strain of its perpendicular diagonal tension member,  $\eta$  can separately be considered as a constant in the integration. Moreover, the application of  $\eta$  is also carried out in the same way of thinking in Vecchio and Collins's study<sup>3</sup>) that  $\eta$  is independently considered and incorporated to the stress-strain relationship for concrete in uniaxial compression.

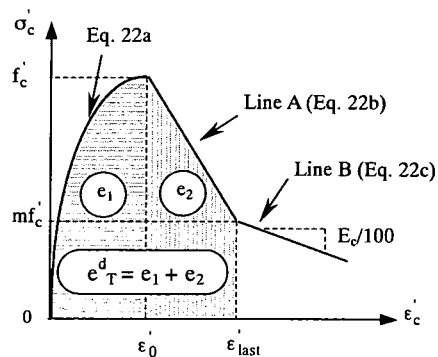


Fig.14 The proposed stress-strain relationship for concrete in compression

## 5. ANALYSIS OF RC DEEP BEAMS

$$e_1 = \int_0^{\varepsilon'_0} \left[ f'_c \left[ 2 \left( \frac{\varepsilon'_c}{\varepsilon'_0} \right) - \left( \frac{\varepsilon'_c}{\varepsilon'_0} \right)^2 \right] \right] d\varepsilon'_c = \frac{2}{3} \varepsilon'_0 f'_c \quad (23)$$

By subtracting  $e_1$  from  $e^d_T$ ,  $e_2$  can be calculated as:

$$e_2 = e^d_T - e_1 = \frac{G_{Fc} L_p}{L} \frac{K_V}{K_E} - \frac{2}{3} \varepsilon'_0 f'_c \quad (24)$$

In addition, by assuming the empirical parameter  $m$  which indicates the stress level of the final failure, the  $\varepsilon'_{last}$  can be derived as:

$$\varepsilon'_{last} = \varepsilon'_0 + \frac{2e_2}{(1+m)f'_c} \quad (25)$$

The value of  $m$  will be considered in the following section.

Therefore, from the obtained parameters, the constant  $A_1$  and  $A_2$  of *Line A* can be calculated as:

$$A_1 = \frac{(m^2 - 1)f_c'^2}{2e_2}; A_2 = f'_c - \frac{(m^2 - 1)f_c'^2}{2e_2} \varepsilon'_0 \quad (26)$$

By assuming the negative slope of *Line B* to be equal to one percent of Young's modulus of the ascending curve, the constant  $B_1$  and  $B_2$  of *Line B* can be determined as:

$$B_1 = -\frac{E_c}{100}; B_2 = mf'_c + \frac{E_c}{100} \varepsilon'_{last} \quad (27)$$

Finally, by substituting the constant  $A_1, A_2, B_1$  and  $B_2$  into **Eq. 22**, the stress-strain curve for concrete members in compression based on the concept of the localized compressive failure can be proposed.

**Figure 15** shows the example simulation of the proposed material model when **case A** is set as the reference. In case that  $f'_c$  is larger, the values of the compressive fracture energy,  $G_{Fc}$ , and  $e_1$  become larger while the value of  $e_2$  is depending on how large  $G_{Fc}$  is, as in **cases B** and **C**. In case of the larger localized compressive failure length,  $L_p$ , the values of  $e_2$  becomes larger. The larger  $L_p$  is, the more gradual drop of load will be predicted as in **case D**. In all cases, the peak point of the proposed material model is fixed at the strain, which is equal to  $\varepsilon'_0$ .

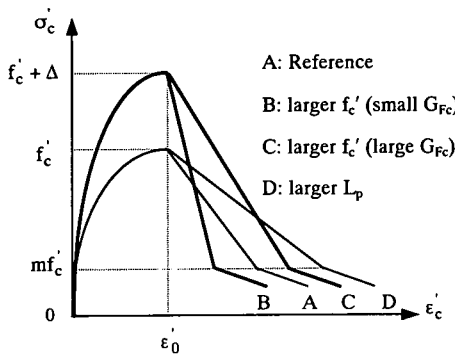


**Fig.15** Simulations of the proposed material model

The experimental data of 6 RC deep beams<sup>2)</sup>, as tabulated in **Table 2**, are adopted and compared with the analytical results using the lattice model and Mander's truss model. All cases of specimens failed in the shear compressive failure mode and the localized compressive failure of concrete was also observed. The lattice model analysis will be discussed first.

Since the failure in a RC deep beam usually takes place in only one side of the beam, it is realized that the analytical model of the full specimen (**Fig. 3**) is more preferable than a half one, which is generally used for simplicity. To apply the proposed concept on localization in compression, the localized compressive failure volume,  $V_p$ , calculated from  $L_p \times A_c$ , must be determined first. It should be recalled that the equation for determining  $L_p$  (**Eq. 15**) of each compression member was derived from the uniaxial compression tests<sup>4)</sup>. If the property of a RC deep beam is homogeneous, due to the externally applied load, the fracture length in both arch members should be equal to  $L_p$ . Thus, the total fracture length is simply considered to be equal to  $2 \times L_p$ . Hence, in the analysis with complete model, one side of arch members should fail with the localized compressive length equal to  $2 \times L_p$ . To simulate the localized compressive failure corresponding to the actual failure behavior in the symmetric model, the compressive strength of an arch member in one side was reduced 0.1% to distinguish their properties.

**Figure 16** shows the comparisons between the experimental and the analytical results by the lattice model in series of  $d = 400$  mm. The experimental results (*Exp.*) are represented by the solid circles. The black thin lines characterize the analytical results when the original equation proposed by Vecchio and Collins (*Original*) has been incorporated to the compression members. The black bold lines represent the analytical results by the complete lattice model incorporating the proposed material model (*Proposed*). For D400, since some part of the post-peak path cannot be captured in the previous study<sup>8)</sup>, the experiment was carried out once more to obtain the complete curve as shown in **Fig. 16(a)**.

It is evident that the analytical results in the pre-peak region express the perfect predictions in most cases. In the post-peak region, the results incorporating the proposed material model show the better and accurate predictions until the ultimate stage compared with ones in which the original equation has been used. It was found that, after some



Table 2 Outline of the experimental data of RC deep beams<sup>2)</sup>

Specimen	b (mm)	a (mm)	d (mm)	h (mm)	$r_w$ (%)	$f_c'$ (MPa)	r	Longitudinal reinforcement*	$p_w$ (%)	$f_y^{**}$ ( $E_s \times 10^5$ )**	Transverse reinforcement	$f_{wy}^{**}$ ( $E_{ws} \times 10^5$ )**
D400	150	400	400	450	0.00	35.7	100	2PC- $\phi$ 25	1.7	1004 (2.00)	-	-
D404					0.42	27.5					D6	331 (2.00)
D408					0.84	38.4					-	-
D600		600	600	650	0.00	40.8	150	2PC- $\phi$ 32	1.8	1006 (2.01)	-	-
D604					0.42	34.2					D6	331 (2.00)
D608					0.84	35.3					-	-

\* : Deformed PC bars      \*\* : Units of  $f_y$ ,  $E_s$ ,  $f_{wy}$ , and  $E_{ws}$  are MPa.

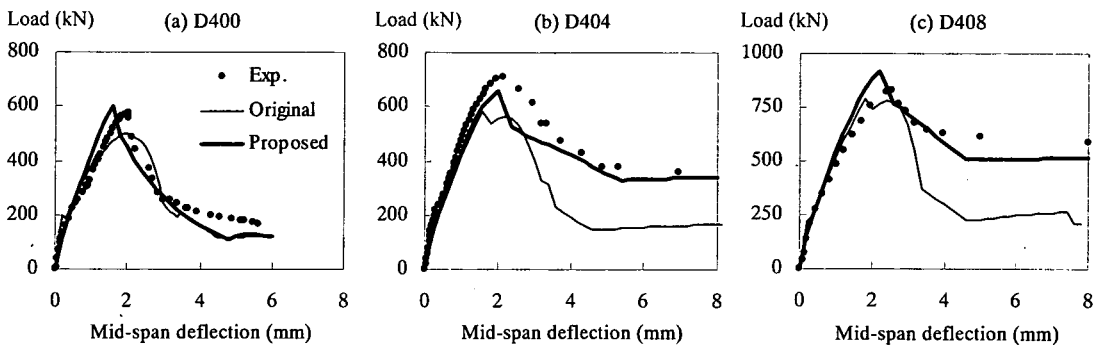


Fig.16 Load and mid-span deflection relationship by the lattice model (d=400 mm)

diagonal compression members in the vicinity of loading point started to express softening behavior, both arch members still provided some resistance for a time and then the RC deep beams were accompanied by the failure of one side of the arch members. Whereas, the other arch member behaved unloading after the maximum load matching with the actual behavior. It should be noted that the diagonal compression members along the diagonal cracks in the side, in which failure did not occur, also provided an additional resistance until the maximum load, while ones in the other side behaved unloading. Conversely, in case that failure is not localized, the techniques in analysis to perform the localization in compression were not employed (i.e. both sides of the beam behave symmetrically in manner). Thus, after some diagonal compression members expressed softening behavior, both arch members failed without any additional resistance from the diagonal compression members as in the above case. Because of this fracture mechanism in the analysis, the shear resisting capacity in this case became slightly lesser than one with the consideration of localization in compression. From the well-predicted analytical results, it implies that the consumed energy is

properly determined and the simple way of considering the fracture length of concrete is appropriate to apply in the complete model analysis.

In Mander's truss model analysis, for simplicity the half models are employed as depicted in Fig. 9. Figures 17 and 18 show the comparisons between the experimental and the analytical results of RC deep beams without and with transverse reinforcement, respectively. The analytical results of Mander's truss model incorporating the proposed material model (*Mander*) are characterized by the black thin lines and compared with the results of the lattice model with the complete model (*Lattice*). The lattice model analysis provides the excellent prediction in the pre-peak region. In the post-peak region, the analytical results of the lattice model express the proper curves corresponding to each experimental result of RC deep beams without and with transverse reinforcement. Although the descending path of D604 and D608 exhibits the snap-back which cannot be expressed in this study, the analytical results present the abrupt energy release as the sudden drop similar to the actual behavior. On the other hand, Mander's truss model provides somewhat difference from the analytical

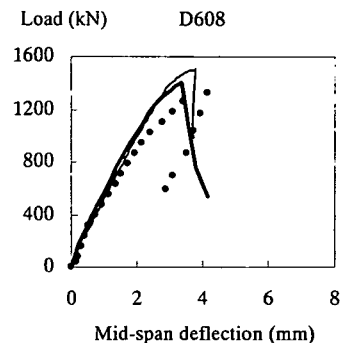
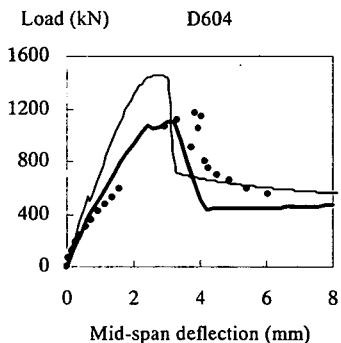
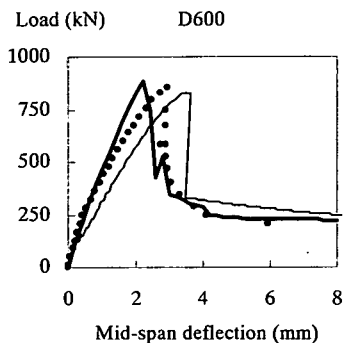
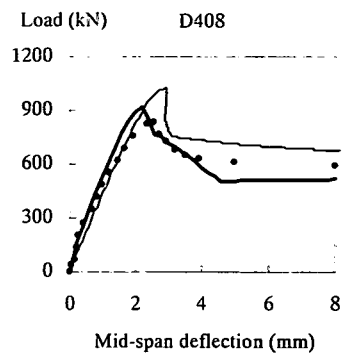
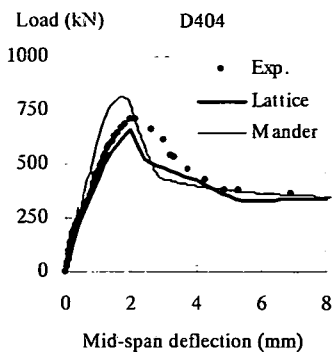
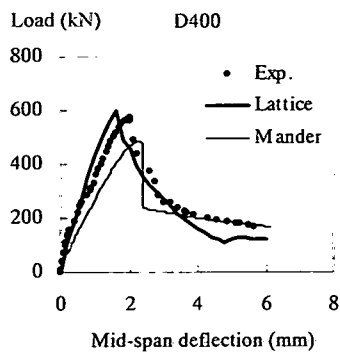


Fig.17 Results of RC deep beams without transverse reinforcement

Fig.18 Results of RC deep beams with transverse reinforcement

results of the lattice model on the shear behavior and the slightly scattering prediction of shear resisting capacity compared with the experimental results. Since inside a RC deep beam it becomes D-region due to its geometrical and statical discontinuity conditions, it is difficult for the simplified model with a small number of members such as Mander's truss model to predict the shear behavior accurately as the lattice model. However, it should be noted that Mander's truss model can evaluate the shear resisting capacity and its deformation within an acceptable degree.

In the analysis, the additional essential parameter,  $m$ , which is the percentage of the level of break point compared with the maximum value in stress-strain curve (Fig. 14), should be considered. Owing to the post peak behavior of the beam is corresponding to the behavior of the arch member, the value of  $m$  for applying to the analysis may relate to the last level of load-deformation relationship from the experimental results. Thus, the value of  $m_e$  in percentage, which is directly assessed from the experimental results by dividing the last level of loading value by the value of the maximum load, and the value of  $m_a$ , which is the parameter  $m$  that gives the best fit of the analytical results to the experimental results, should be considered. Figure 19 shows that the parameters

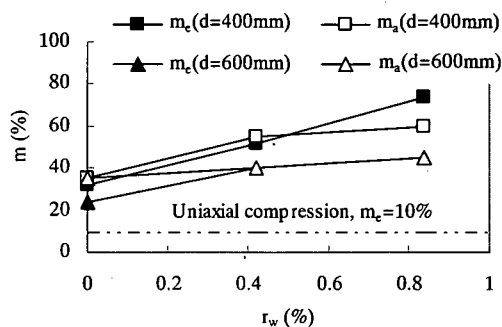


Fig.19 Relationships of  $m$  with  $r_w$  and  $d$

$m_e$  and  $m_a$  are depending on the effective depth and the transverse reinforcement ratio. It indicates that the values of  $m_e$  and  $m_a$  are different in some case. The effect of the existence of reinforcement inside is considered as the reason to cause this difference.

From Fig. 19, the possible reason for the difference in values of  $m_e$  from RC deep beams and uniaxial compression tests<sup>4)</sup> is the effects of the internal stress due to reinforcement and secondary cracks occurring in RC deep beams. However, the value of  $m$  represents the level in which the slope of load-deformation curve becomes horizontally flat. This means the calculation of the consumed energy by compression concrete members was assumed to

be based on the occurrence of the major crack excluding the effect of the secondary cracks. Moreover, by considering the tied arch in RC deep beams, the load is transmitted directly to the supports by concentrated unidirectional compression forces in concrete. Therefore, the concepts of localization in compression from the uniaxial compression tests are still applicable for RC deep beams.

Based on the limited number of values of  $m_a$ , the values of  $m$  to be used in the analysis is proposed as:

$$m = -3\left(\frac{2400}{d} - 3\right)r_w^2 + 13\left(\frac{2400}{d} - 3\right)r_w + 35 \quad (\%) \quad (28)$$

where the units of  $r_w$  and  $d$  are percent and mm, respectively. It was found that when the value of  $m$  changes 1%, even though the compression softening factor,  $\eta$ , is not incorporated, the difference in calculated values of load in the post-peak region are only 1% of the maximum values in all cases. Hence, if the applied value of  $m$  is not extremely different, the difference of the analytical results in the post-peak region can be neglected. Moreover, based on the tendency of the analytical results and the applied values of  $m$ , the applicable range of Eq. 28 is suggested for the RC deep beams ( $a/d=1$ ) where  $d$  is varied from 400 to 600 mm and  $r_w$  is varied from 0 to 1.0%. Nevertheless, due to the application of  $m$  is recommended based on the limited experimental data, more experimental data are required in order to obtain more reliable relationship in the further study.

## 6. CONCLUSIONS

In the shear analysis of RC deep beams, where the whole member becomes D-region due to the concentrated unidirectional compression along the diagonal struts, even though there are some effects due to the existing of reinforcements, the concepts on localized compressive failure from the uniaxial compression tests are considered to be still applicable. The empirical parameters of localization in compression, such as the localized compressive failure length,  $L_p$ , and the compressive fracture energy,  $G_{Fc}$ , are applied to formulate the compressive stress-strain relationship of concrete. The proposed material model consists of the parabolic equation with the consideration of compression softening proposed by Vecchio and Collins<sup>3)</sup> in the ascending branch and, in the descending branch, the bilinear equation which is formulated from the consumed energy by the failed concrete.

For RC deep beams with and without transverse reinforcement failed by the localized compressive failure of concrete, the incorporation of concept on the localization in compression in the analysis provides the superior accurate prediction, especially in the post-peak region, compared with those in which this concept is not considered.

Since the failure of RC deep beams occurs locally in one side of the beam, the complete model of the lattice model with the computational technique in property distinction of both arch members is recommended to yield the prediction matching the actual behavior. It is evident that the lattice model incorporating the proposed material model yields the excellent prediction on the shear behavior until the ultimate stage and the trustworthy shear resisting capacity. Alternatively, with the proposal in the consideration of the shear resistance due to the strut along the diagonal crack, Mander's truss model, in which the number of degree of freedom is smaller than the lattice model, provides the satisfactory results of load-deformation relationship.

## REFERENCES

- 1) Schlaich, J., Schäfer, I. and Jennewein, M.: Towards a consistent design of structural concrete, *Journal of PCI*, Vol. 32, No. 3, pp.74-150, 1987.
- 2) Lertsrisakulrat, T., Niwa, J., Yanagawa, A. and Matsuo, M.: Concepts of Localized Compressive Failure of Concrete in RC Deep Beams, *Journal of Materials, Concrete Structures and Pavements, JSCE*, No. 697/V-54, pp.215-225, Feb. 2002.
- 3) Vecchio, F.J. and Collins, M.P.: The Modified Compression Field Theory for Reinforced Concrete Elements Subjected to Shear, *ACI Structural Journal*, Vol. 83, No.2, pp.219-231, 1986.
- 4) Lertsrisakulrat, T., Watanabe, K., Matsuo, M. and Niwa, J.: Experimental Study on Parameters in Localization of Concrete Subjected to Compression, *Journal of Materials, Concrete Structures and Pavements, JSCE*, No. 669/V-50, pp.309-321, Feb. 2001.
- 5) Niwa, J., Choi, I.K. and Tanabe, T.: Analytical Study on Shear Resisting Mechanism of Reinforced Concrete Beams, *Journal of Materials, Concrete Structures and Pavements, JSCE*, No.508/V-26, pp.79-88, Feb. 1995.
- 6) Mander, J.B., Kim, J.H. and Dutta, A.: Shear-Flexure Interaction Seismic Analysis and Design, *Modeling of Inelastic Behavior of RC Structures Under Seismic Loads*, ASCE, pp.369-383, 2001.
- 7) Niwa, J.: Equation for Shear Strength of Reinforced Concrete Deep Beams Based on FEM Analysis, *Concrete Library of JSCE*, No.4, pp.283-295, 1984.
- 8) Lertsamattiyakul, M., Lertsrisakulrat, T., Miki, T. and Niwa, J.: RC Deep Beam Analysis Considering Localization in Compression, *Proceedings of the JCI*, Vol. 24, No.2, pp.943-948, 2002.

(Received July 1, 2002)

お詫びと訂正

土木学会論文集 No. 711/V-56 (2002年8月号)

Tamon UEDA, Yasuhiko SATO, Tsunemasa ITO and Katsuhide NISHIZONO  
 “SHEAR DEFORMATION OF REINFORCED CONCRETE BEAM”

の209頁の図に誤りがありましたので、下図のように訂正し、お詫び致します。

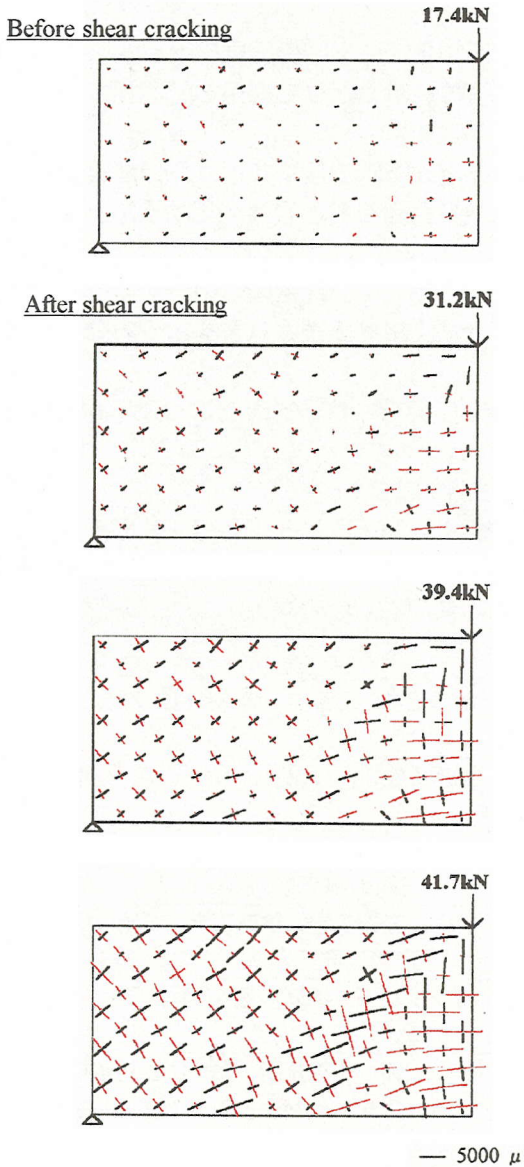


Fig.9 Principal strain distribution for specimen No.1

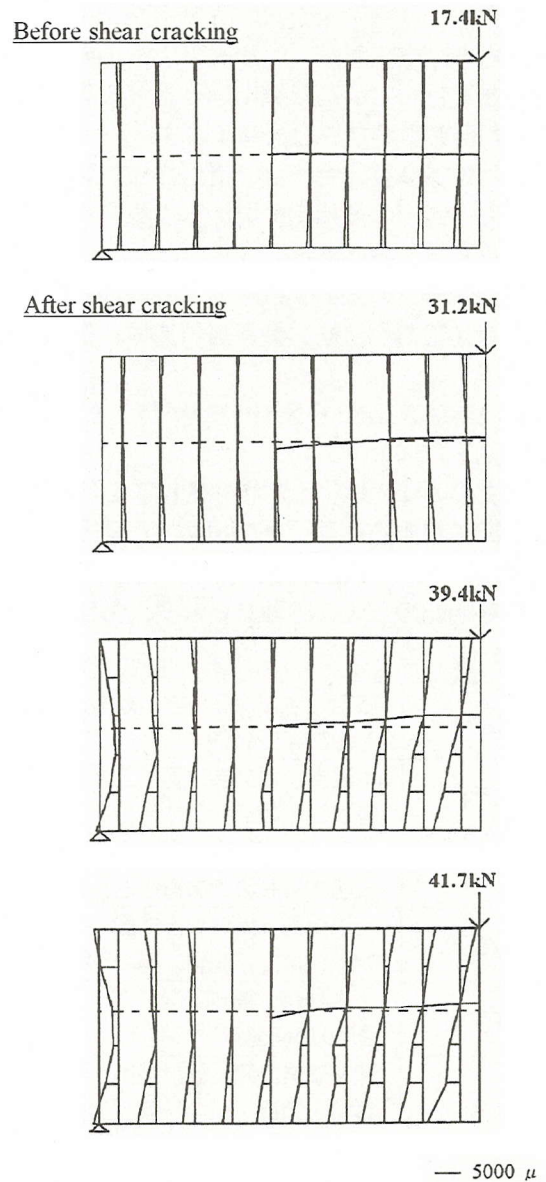


Fig.10 Normal strain in direction of member axis and neutral axis for specimen No.1